Long-day photoperiods affect expression of OPN5 and the TSH-DIO2/DIO3 pathway in Magang goose ganders

Jian-qiu Pan,[*,†,‡] Sui Liufu,[†,‡] Jun-feng Sun,[†,‡] Wen-jun Chen,[†,‡] Hong-jia Ouyang,[†,‡] Xu Shen,[†,‡] Dan-li Jiang,[†,‡] Dan-ning Xu,[†,‡] Yun-bo Tian,[†,‡] Jian-hua He ⬤,[*] and Yun-mao Huang[†,‡,1]

[*]College of Animal Science and Technology, Hunan Agricultural University, Changsha 410128, China; [†]College of Animal Science & Technology, Zhongkai University of Agriculture and Engineering, Guangzhou 510225, China; and [‡]Guangdong Province Key Laboratory of Waterfowl Healthy Breeding, Guangzhou, Guangdong 510225, China

ABSTRACT This study sought to understand the regulation mechanism of OPN5 through the TSH-DIO2/DIO3 pathway mediated photoperiod on the breeding activity of short-day breeding birds. In this study, the reproductive activity of Magang goose was regulated by artificial light, and the reproductive activity of the ganders were determined according to the daily laying rate of female geese. The testicular development and the serum reproductive hormone concentrations of ganders were measured during the reproductive period (d 0), the reproductive degeneration period (d 13 and 27) and the resting period (d 45). The mRNA and protein expression patterns of OPN5, the HPG axis reproductive genes, and TSH-DIO2/DIO3 pathway related genes were examined. Results showed that the laying rate of geese and the gonadal indices (**GSI**) decreased gradually after the photoperiod increased. Histological observation found that the spermatogenic function of the testis was normal on d 0 and 13, while degeneration occurred by d 27 and 45. Serum testosterone, FSH, and LH concentration showed a slight increase on d 13, followed by a sharp decrease on d 27 and 45 ($P < 0.01$), while PRL concentrations were low on d 0 and 13, and increased rapidly on d 27 and 45 ($P < 0.01$).The expression pattern of *GnRH, FSH, LH,* and *THRβ* mRNA were similar, with high levels on d 0 and 13 and a decreasing trend on d 27 and 45 ($P < 0.05$ or $P < 0.01$); and *GnRHR* mRNA levels were higher on d 13 ($P < 0.05$), but then had decreased by d 27 and 45 ($P < 0.01$). The expression pattern of *GnIH* and *GnIHR* was similar, which was opposite to that of *GnRHR*. *VIP, PRL*, and *PRLR* increased gradually and peaked on d 45 ($P < 0.01$). The expression trend of *TRH, TSHβ*, and *DIO2* was similar to that of *GnRHR*, and the expression abundance increased on d 13, and then decreased on d 27 and 45. GnRH protein expression was significantly higher than during the other 3 periods ($P < 0.01$) while the GnIH protein levels were extremely low on d 0, had gradually increased by d 13, and significantly increased by d 27 and 45 ($P < 0.01$). The protein expression trends of THR and DIO2 were similar to that of GNIH. DIO3 protein expression was low on d 0 and 13, and increased by d 27 and 45. These results suggest that when the photoperiod increased, the hypothalamus OPN5 gene and protein were upregulated and the pituitary TSHβ, TSHR, and hypothalamus THRβ, TRH, and DIO2 were downregulated, and thus the reproductive activity of geese was inhibited.

Key words: Magang goose, OPN5, TSH-DIO2/DIO3 pathway, HPG axis, photoperiod

INTRODUCTION

Most birds are seasonal breeders. Under natural conditions, their reproductive status adjusts for breeding and non-breeding periods in response to annual photoperiodic rhythms (Tamai and Yoshimura, 2017; Nakane Yusuke, 2019; Liu et al., 2020). Studies have shown that light signals are converted into hormonal signals through photoreceptors acting on the hypothalamus; these hormones regulate reproductive activities of birds through a series of signal transduction and endocrine systems (Li et al., 2009; Dardente et al., 2014). These photoreceptors are opsins, such as neuropsin (**OPN5**), melanopsin (**OPN4**), and vertebrate ancient-opsin (**va-OPN**; Shichida and Matsuyama, 2009; Kang and Kuenzel, 2015; Kuenzel et al., 2015). Upon activation of these photoreceptors, light signals further affect the production of thyroid stimulating hormone (**TSH**) in the pars tuberalis (**PT**). In long-day breeding birds, TSH secreted by the PT acts on the tanycyte of the

hypothalamus to express type II deiodinase (**DIO2**) and convert thyroxine (**T4**) into biologically active triiodothyronine (**T3**), which regulates the synthesis and secretion mechanism of GnRH/GnIH in the hypothalamus and regulates the secretion of pituitary gonadotropin (Dawson et al., 2001; Ikegami and Yoshimura, 2012; Shinomiya et al., 2014; García-Fernández et al., 2015).

OPN5 is one of the major deep brain photoreceptors (**DBPs**) in birds, and is involved in mediating photoperiod regulation of their seasonal reproduction (Nakane et al., 2010; Kang and Kuenzel, 2015). In a study of canaries, the knockdown of OPN5 via small interfering RNA antisense in the MBH promoted the expression of TSHβ (Stevenson and Ball, 2012). However, it was found in quail that the decrease of OPN5 mRNA significantly inhibited the expression of long-day-induced TSHβ mRNA (Nakane et al., 2014). In addition, a study of Blonder white geese found that the expression abundance of OPN5 increased when light duration was extended from 8 to 11 or 14 h, but the geese laid better under 11 h light, and the expression abundance of OPN5 was higher than that of L14, while the TSHβ expression abundance of L11 was lower than that of L14 (Zhu et al., 2019). However, in the study of Yangzhou geese, OPN5 expression was positively correlated with TSH and DIO2. OPN5 was upregulated with prolonged light exposure and the relative abundance of OPN5 expression under white and red light was higher than that under blue and green light, which promoted the geese's laying performance (Zhu et al., 2019). In Pekin ducks, OPN4, OPN5, and GnRH increased before the increase in gonadal steroids and onset of laying, and maintained high levels during the laying period (Van Wyk and Fraley, 2021). Moreover, the expression of OPN5 in the hypothalamus of quails varied with age. Immature quails have low levels of OPN5 in the hypothalamus but significantly increased OPN5 expression in mature (6 wk) and adult (16 wk, sexually active) quails, with peaks during the adult stage, and then a significant decrease in aged (144 wk) quail (Banerjee et al., 2018). The testis of quail degenerated under different photoperiodic conditions (photosensitive, scotorefractory, photorefractory, and scotosensitive), and the number of ir-OPN5 cells in the paraventricular organ (**PVO**) decreased significantly (Banerjee and Chaturvedi, 2017).

The aforementioned studies suggest that OPN5 in birds transmits light signals to the PT, which initiates the thyroid hormone response (TH-responsive) signaling pathway and initiates the hypothalamic-pituitary-gonadal axis (**HPGA**) through T3, which regulates reproduction in birds. However, the expression patterns of OPN5 and the TSH-DIO2/DIO3 pathway are different in different breeding types and different breeding states. And most of the studies on photoperiodic regulation of seasonal breeding activity in birds have been conducted on long-day breeding birds; few have been conducted on short-day breeding birds. Magang geese are typical short-day breeding birds, and the seasonal variation of their breeding activities is mainly regulated by light. Long light inhibits the reproductive activity of Magang geese, while short light promotes it (Huang et al., 2008). In the present study, the reproductive activities of Magang geese were divided into the non-breeding period and the breeding period. From April to July, the reproductive activities of Magang geese were inhibited or stationary during the non-breeding period. August to March of the following year is the breeding period. During the breeding period, the geese will have nested 4 to 5 times, when their reproductive activity is suppressed and production is stopped (Shi et al., 2007; Zhu et al., 2017). In the present study, the reproductive activity of Magang goose ganders was regulated by artificial light, and the expression patterns of OPN5 and the TSH-DIO2/DIO3 pathway in different reproductive states was explored to understand the regulation mechanism of OPN5 on the reproductive activity of Magang geese through the TSH-DIO2/DIO3 pathway.

MATERIALS AND METHODS

Experimental Design and Animals

The experiment was carried out at Shanwei city (115° E, 13°N), Guangdong Province over 45 d, starting on the January 26, 2021. Magang geese at 1 yr of age (n = 480, ♂:♀=1:5) and of the same genetic origin were selected and reared in an automatically light-controlled shed with a feeding density ≥ 0.3 m^2 per goose. The shed has a playground (15 × 12 m) and 2 baths (3.5 × 5 m). Over the experimental period, the geese were fed a restricted diet (150 g/d) of egg duck feed and green grass, and ad lib drinking water. Before the experiment, the geese were kept under short light (12L:12D) for 2 mon so that the flock was in the breeding period, during which the egg production rate was $\geq 10\%$. Geese were exposed to short-day light (12L:12D) on d 0 which from d 1 was gradually extended (2 h/d) to 18 h (18L:6D)—this light regime was continued to the end of the experiment. The eggs of the female geese were collected daily to calculate laying rate, which was used to indicate the reproductive activity of the ganders.

This study was carried out in strict accordance with the recommendations in the Guide for the Care and Use of Laboratory Animals of Zhongkai University of Agriculture and Engineering (NO.2020122501). The protocol was approved by the Committee on the Ethics and Welfare of Animal Experiments of Zhongkai University of Agriculture and Engineering. All efforts were made to minimize suffering of the animals.

Tissue Collection, Microscopy, and Histological Evaluation

Eight ganders at the breeding stage (d 0), reproductive regression stage (d 13 and 27), and resting period (d 45) were randomly selected to be weighed and have blood samples taken. The ganders were then decapitated and the hypothalamus and pituitary were harvested and frozen in liquid nitrogen for test gene and protein

expression. The testicular tissue was collected and weighed. The right testis was collected and frozen in liquid nitrogen to test for gene expression. The left testis were collected and fixed in 4% paraformaldehyde solution for more than 24 h. The testis was then dehydrated by gradient alcohol in the automatic dehydrator (YD-14P, Jinhua Yidi, China). The tissues were embedded in the embedding machine and 6-μm-thick sections were cut using the paraffin slicer (YD-355AT, Jinhua Yidi) and stained with hematoxylin-eosin. All samples were included for histologic analysis, and the changes of seminiferous tubules and spermatogenic cells were observed under the microscope (ECLIPSE E100, Nikon, Tokyo, Japan).

Observation and analysis of testicular section: 5.0 × and 10.0 × testicular tissue was extracted from Case Viewer, and image-pro Plus 6.0 analysis software was used to measure the area of 5 convoluted tubules (mm^2) in 5.0 × screenshots of each section, using mm as the standard unit. The thickness of spermatogenic epithelium in 8 circular seminiferous tubules was measured (μm) in 10.0 × screenshots of each section.

Blood Sample Collection and Hormone Determination

Blood samples were collected from the wing vein of 8 randomly selected male geese at d 0, 13, 27, and 45. The serum was separated by centrifuging the blood at 3,000 g within 3 h of sample collection. The serum was then stored at −20°C until reproductive hormone concentrations were measured. Serum testosterone concentrations were measured using a universal immune assay enzyme

kit (Elabscience, China) following the manufacturer's protocol. Serum follicle-stimulating hormone (**FSH**), luteinizing hormone (**LH**), and prolactin (**PRL**) levels were measured using chicken- or duck-specific immune assay enzyme kits (SAB) following the manufacturer's protocol. The sensitivity of each assay was 0.17 ng/mL, 0.6 mIU/mL, 0.5 mIU/mL, and 20 μIU/mL for testosterone, FSH, LH, and PRL, respectively. The intra- and interassay variation coefficients were all below 15%, and the R-values for the standard curves were greater than 0.99 for these assays.

RNA Isolation, cDNA Synthesis, and Quantitative Real-Time Polymerase Chain Reactions

Real-time quantitative polymerase chain reaction (**qRT-PCR**) was performed for quantification of *OPN5*, thyrotropin releasing hormone (**TRH**), thyroid hormone receptor beta (**THRβ**), *TSHβ*, thyroid stimulating hormone receptor (**TSHR**), *DIO2*, *DIO3*, *GnRH*, *GnIH*, vasoactive intestinal peptide (**VIP**), *FSHβ*, LHβ, and *PRL* mRNA expression levels in the hypothalamus or pituitary. Total RNA was extracted from the hypothalamus and pituitary using TRizol (Invitrogen). The cDNA was synthesized using the Rever Tra Ace qPCR RT Master Mix with gDNA Remover (Toyobo, Japan), following the recommended manufacturer's protocol. Based on the reference sequence on NCBI, the primers for the above genes and the internal reference β-actin gene were designed using Primer 5. 0 (Table 1) and synthesized using Sangon Biotech Co., Ltd. Using cDNA as

Table 1. Pimers used in the real-time quantitative PCR assay of the genes.

Gene name	Primer sequence (5′-3′)	Annealing temperature (°C)	PCR products (bp)	Accession number
OPN5	F: ACCAGGATCCAGAACAGCCA R: GCAATGAGGAATCCGGCACA	60	80	KM922545.1
TRH	F:TGGTGAAGTAAATTGCCAGAACAC R: CCTAAATGGGGACACTCACTCAC	60	106	XM_013182272.1
THRβ	F: GCTTATCTCTGGGCAATGTGAC R: TTGAAGCGACATTCCTGGCA	60	299	XM_038174583.1
TSHβ	F:CGTGTGCACATACAAAGAGAT R: GCAATAGTTTGGCCTAACCTT	60	162	NM_001310425.1
TSHR	F: TGTTAACTGCCTATGCGCCA R: CCGGTCAGGATGGTAGAAGC	60	200	XM_009646634.2
DIO2	F:GACGCCTACAAGCAGGTCAA R: GTTCCACACTTGCCACCAAC	57	119	XM_013194618.1
DIO3	F:TGGGCTTAAAGAGAAGCGGG R: CTAGGAGCCAGAGCATCACG	57	214	XM_013199473.1
GnRH	F: CTGGGACCCTTGCTGTTTTG R: AGGGGACTTCCAACCATCAC	59	209	NM_001080877.1
GnIH	F: AAAGTGCCAAATTCAGTTGCT R: GCTCTCTCCAAAAGCTCTTCC	58	128	XM_015853673.2
VIP	F: CTGGGAAACAGACTGCCCTT R: GACTGTCCTGGGAGCTATCAAT	56	132	XM_013178195.1
FSHβ	F: GTGGTGCTCAGGATACTGCTTCA R: GTGCAGTTCAGTGCTATCAGTGTCA	60	209	XM_031607398.1
LHβ	F: CCAGGCCTCCTGCACCTAC R: GGCGCAGCGGCAGCTCAG	60	115	MK820637.1
PRL	F: ACCTCCTTGCCTATCTGCCC R: TTGTAATGAAACCCCGACCC	60	136	XM_013184821.1
β-actin	F: CCTCTTCCAGCCATCTTTCTT R: TGTTGGCATACAGGTCCTTAC	56	110	XM_035563367.1

a template, a 10-μL reaction system was prepared with the following: Master Mix (5 μL), upstream and downstream primers each of 0.1 μL, ddH$_2$O (3.8 μL), and a cDNA template (1 μL). Reaction conditions were set as: 50°C pre-denaturation for 2 min, then 95°C for 10 min, then 95°C for 15 s, then the annealing temperature (°C) for 1 min, for 40 cycles. Three replicates of each sample were corrected with β-actin as an internal reference gene. The results were processed using the relative template volume algorithm ($\Delta\Delta$Ct method), and the relative gene expression was characterized as $2^{-\Delta\Delta Ct}$.

Protein Expression Detection

Total hypothalamus protein was extracted and protein expression of OPN5, THRβ, DIO2, DIO3, GnRH, and GnIH was detected. The BCA assay method was used to quantify the total protein contents of the hypothalamus tissue. The total proteins were loaded in the SDS PAGE sample buffer and the components were separated using 10% SDS-PAGE. Proteins were transferred to a PVDF membrane (Thermo Scientific, Waltham, MA., USA, Cat No. 88518) by wet blotting, and then the membranes were blocked for 2 h at room temperature with 5% non-fat milk in PBS containing 0.05% Tween-20 (PBS-T). After blocking, the blots were incubated over night at 4°C with diluted primary antibodies against OPN5 (self-madepolyclonal antibody, 1:1,000), THRβ (Invitrogen, Carlsbad, CA, 1:1,000), DIO2 (Proteinech, Wuhan, China, 1:1,000), DIO3 (ABclonal, Wuhan, China, 1:1,000), GnRH (Affinity, OH, 1:1,000), and GnIH (self-made polyclonal antibody, 1:1,000) antibodies. The membrane was then washed 5 times in tris-buffered saline with Tween-20 (0.1%) and incubated with an HRP-conjugated goat anti-rabbit or goat anti-mouse secondary antibody (Affinity and Abcam,Cambridge, UK, 1:10,000) for 1 h at room temperature. The membrane was again washed 5 times for 3 min each time, and finally the immunoreactive proteins were detected using an enhanced chemiluminescence western blotting detection kit (GLPBIO, CA). The β-actin protein served as an internal control (Proteinech, 1:1,000).

The rabbit polyclonal antibodies of anti-OPN5 and anti-GnIH were generated by using synthetic peptides (OPN5: KLH-CISSHRDSAALSETQLEV, GnIH: KLH-CSIKPIANLPLRF) according to the preparation method of previous studies (Nakane et al., 2010; Kojima et al., 2011; Mohsin et al., 2020).

Statistical Analysis

Data are presented as the mean $\pm$ standard error. Data were analyzed by one-way analysis of variance, using the Statistical Package for Social Sciences (**SPSS**) version 19.0, and the means were considered significantly different at $P < 0.05$ and highly significantly different at $P < 0.01$. The western blot protein bands were analyzed for grayscale values using Image J software.

RESULTS

Effects of Long-Day Photoperiods on Reproductive Activity and Testicular Development in Geese

During the course of the experiment, the egg-laying rate of female geese decreased gradually with increasing light duration and had stopped on d 30 (Figure 1A). The reproductive status of ganders was determined according to the egg production of female geese, and samples were taken on d 0 (breeding period), d 13 and 27 (reproductive regression period), and d 45 (resting period). The GSI decreased gradually and was highly significantly different on d 45 ($P < 0.01$; Figure 1B). Histological observation of the testis revealed that at the beginning of the experiment (d 0), the ganders were in the reproductive phase, the testicular varicose tubules were intact, the spermatogenic cells of all grades in the tubules were abundant, and a large number of spermatozoa were visible in the center of the tubular lumen. After 13 d of light addition, the situation of seminiferous tubules and spermatogenic cells were similar to that of d 0, but the number of spermatocytes in the central part of the tubules was slightly reduced. Twenty-seven days later, the lumens of the seminiferous tubules were dilated, and the number of spermatogenic cells at all levels and the spermatozoa were reduced. After 45 d, the testis had completely degenerated, the area of seminiferous tubules was significantly reduced, the wall of tubules was thickened, and there were a large number of sertoli cells in tubules. Spermatogenic cells and spermatozoa at all levels were almost invisible (Figure 1C). Further analysis of the area of seminiferous tubules and the thickness of spermatogenic epithelium in different periods showed that the area of seminiferous tubule on d 0 and 13 was similar, while the area of seminiferous tubule on d 27 and 45 was lower than that on d 0 and 13 ($P < 0.01$ or $P < 0.05$; Figure 1D). The thickness of the spermatogenic epithelium was highly significantly reduced throughout the test period ($P < 0.01$; Figure 1E).

Hormone Concentrations in Serum

Under the short-day photoperiod condition (d 0), serum testosterone concentrations were at a high level with concentrations of 4.25 ± 0.52 ng/mL, and then decreased highly significantly ($P < 0.01$) on d 27 and 45, with concentrations of 1.79 ± 0.18 and 0.74 ± 0.07 ng/mL, respectively (Figure 2A). Serum FSH concentrations were significantly increased ($P < 0.01$) on d 13, but decreased significantly at d 27 and 45 (Figure 2B). Serum LH levels were similar on d 0 and 13, while LH levels were highly significantly lower ($P < 0.01$) on d 27 and 45 (Figure 2C). Serum PRL levels were significantly decreased ($P < 0.05$) after d 13 of altered light, while the PRL levels were highly significantly increased ($P < 0.01$) on d 27 and 45 (Figure 2D).
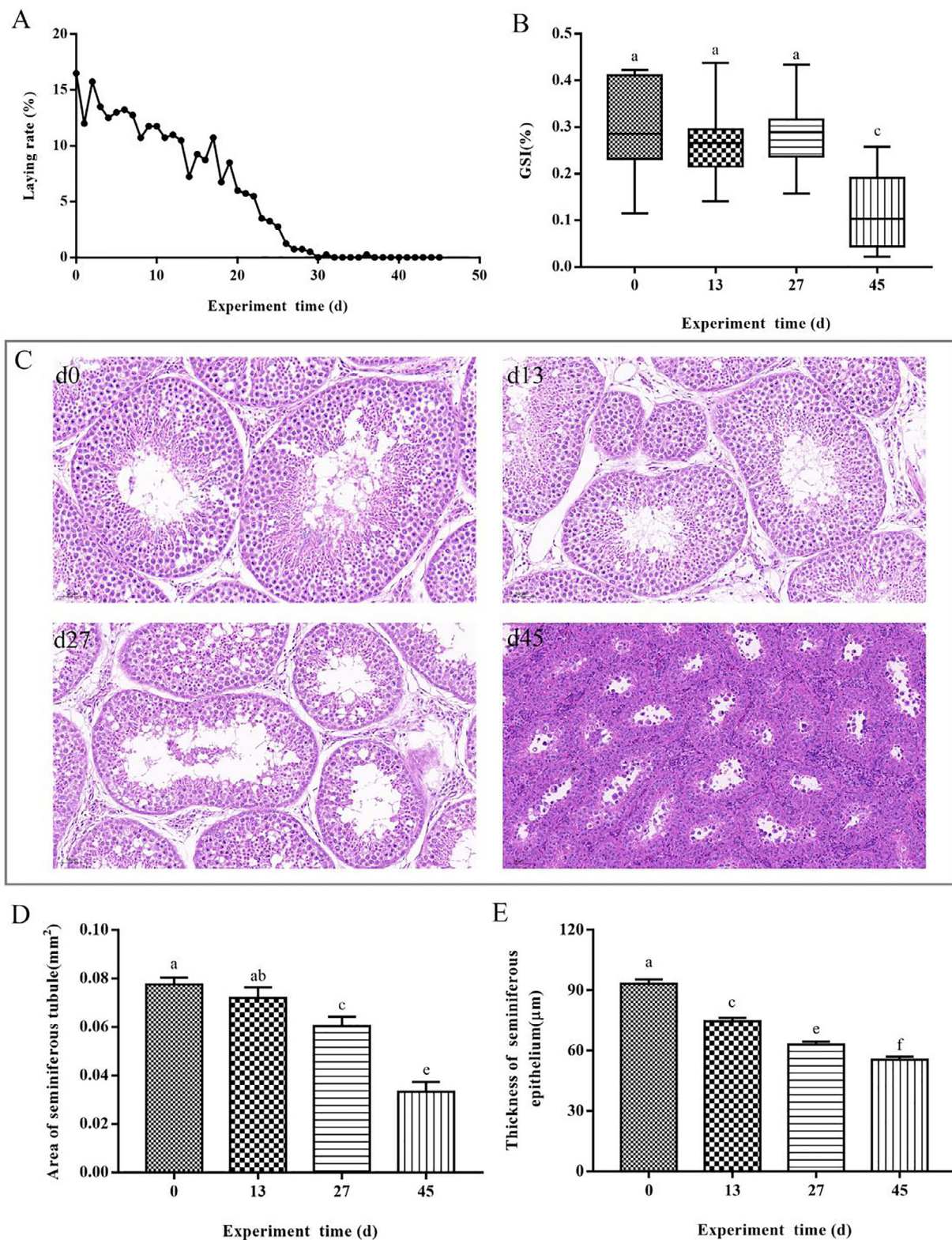
Figure 1. Laying rate, GSI, and the histological observation and analysis of testis. (A) Daily laying rate of geese and the artificial photoperiodic programs. (B) The GSI of ganders. (C) Histological analysis of sections from ganders testes. Scale bar represents 50 μm at 20 × magnification. (D, E) The area of seminiferous tubules (mm^2) and thickness of seminiferous epithelium (μm) were obtained by Image-Pro Plus 6.0 software. Consecutive letters (e.g, a, b) indicate significant differences ($P < 0.05$), and discrete letters (e.g, a, c) indicate highly significant differences ($P < 0.01$), the same as below. Abbreviation: GSI, gonadal indices.

Expression of HPG Axis-Related Genes and Proteins

In the hypothalamus, *GnRH* mRNA expression levels (Figure 3A) were at similarly high levels on d 0 and 13 and had significantly decreased by d 27 and 45 ($P < 0.01$). Throughout the experimental period, the expression pattern of *GnIH* mRNA (Figure 3B) was opposite to that of *GnRH*, with lower expression abundance on d 0 and 13, while *GnIH* expression was
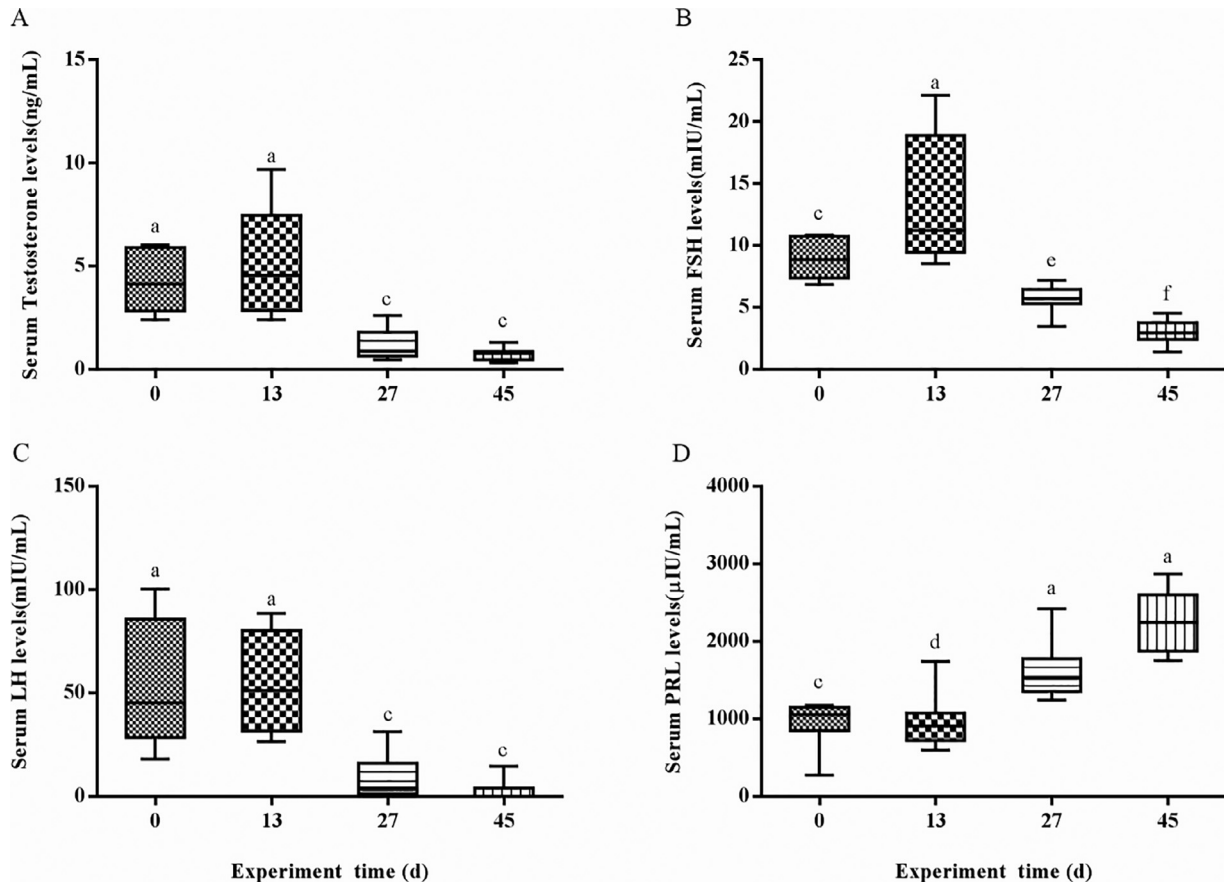
Figure 2. Serumreproductive hormone levels. (A−D) The levels of testosterone, FSH, LH, and PRL reproductive hormones, respectively. Abbreviations: FSH, follicle-stimulating hormone; LH, luteinizing hormone; PRL, prolactin.

significantly higher on d 27 and 45 relative to d 13 ($P < 0.05$). The expression abundance of *VIP* mRNA (Figure 3C) was at similarly low levels on d 0, 13, and 27, but had significantly increased on d 45 ($P < 0.01$). In the pituitary, the *GnRHR* mRNA levels (Figure 3D) were significantly higher on d 13 ($P < 0.05$) and then significantly decreased on d 27 and 45 ($P < 0.01$), with a trend similar to that of *GnRH*. The changing trend of *GnIHR* mRNA (Figure 3E) was also similar to that of *GnIH*, with a lower level of gene expression on d 0 and 13, followed by significant increases on d 27 and 45 ($P < 0.05$ or $P < 0.01$). The gene expression trends of *FSH* and *LH* (Figures 3G and 3H) were similar; they maintained a high level on d 0 and 13, and then decreased significantly on d 27 and 45 ($P < 0.01$). The trend of *PRL* and *PRLR* mRNA expression (Figures 3F and 3I) was similar to that of hypothalamic *VIP*, which gradually increased with the duration of the experiment and showed a highly significant increase on d 27 and 45 ($P < 0.01$). In addition, the protein expression of GnRH was highest on d 13 and significantly higher than at the other three times ($P < 0.01$). However, the GnIH protein levels were extremely low on d 0, gradually increased after long-day photoperiod exposure, and significantly increased on d 27 and 45 ($P < 0.01$, Figures 3J and 3K).

Protein and mRNA Expression for Both OPN5 and the TSH-DIO2/DIO3 Pathway Genes in Long Day Conditions

The relative expression of *OPN5* mRNA (Figure 4A) was significantly increased on d13, 27, and 45 ($P < 0.05$ or $P < 0.01$), peaking on d 27. The results of the OPN5 protein (Figures 4H and 4I) also showed that the protein level of OPN5 was significantly higher on d 13, 27, and 45 than on d 0 ($P < 0.01$). The expression abundance of *DIO2* mRNA (Figure 4B) in the hypothalamus was expressed at the highest level on d 13 and was highly significantly higher than that on d 0, 27, and 45 ($P < 0.01$). This result was similar to the protein expression trend of DIO2 (Figures 4H and 4I), but the protein expression level of DIO2 was also higher on d 0, which was significantly higher than that on d 27 ($P < 0.05$). The expression trends of the *DIO3* genes (Figure 4C) and proteins (Figures 4H and 4I) were generally consistent, with lower expression levels on d 0 and 13, higher values on d 27 and 45, and significant increased on d 45. The *THRβ* mRNA (Figure 4D) was at a high level on d 0 and 13, while its expression abundance was significantly decreased on d 27 and 45 ($P < 0.05$ or $P < 0.01$). This result was generally consistent with the results of THR protein expression
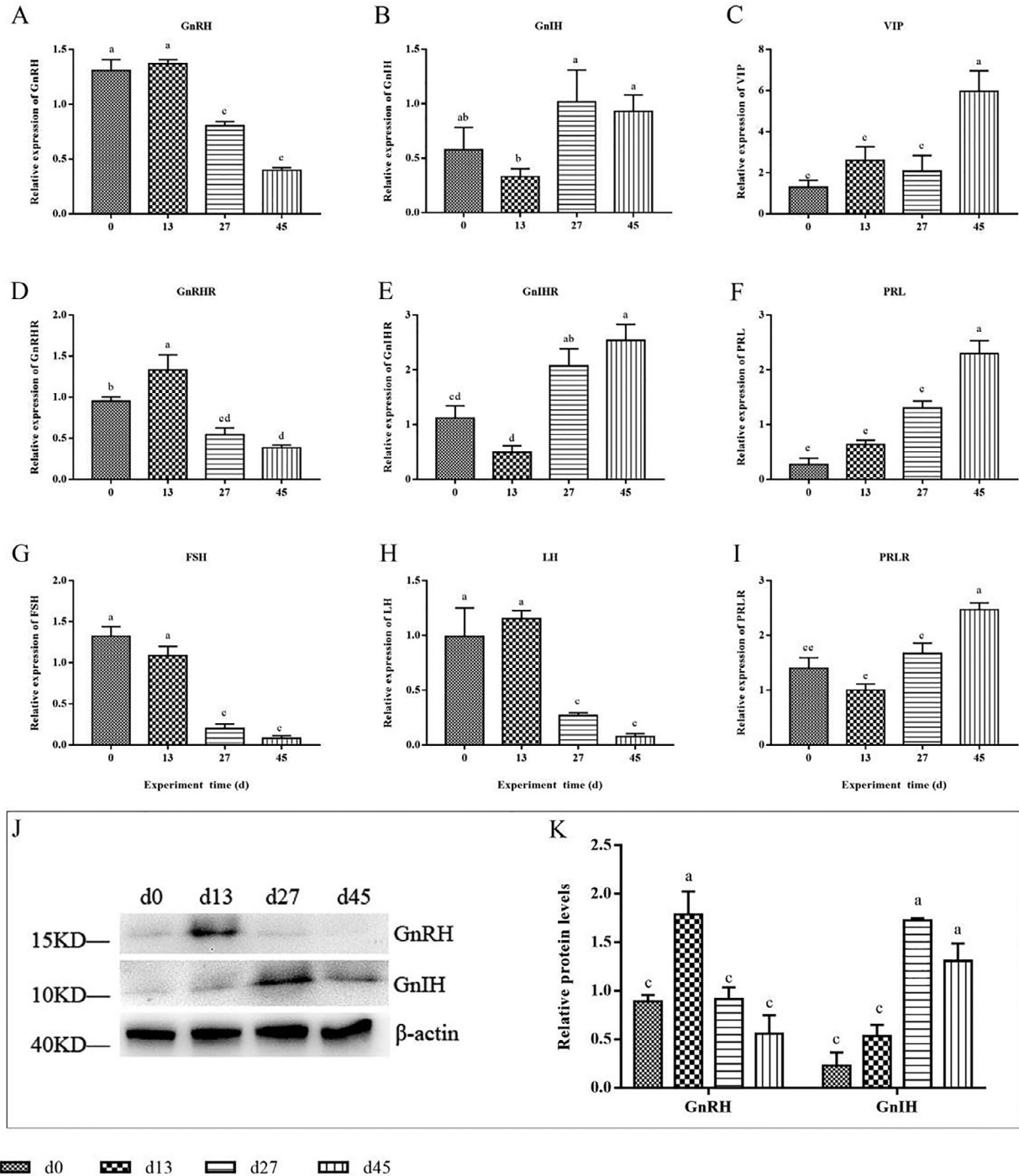
Figure 3. Expression of HPG axis-related genes and proteins. (A–C)The relative abundances of mRNA for hypothalamic *GnRH, GnIH, VIP*, respectively. (D–I) The relative abundances of mRNA of the pituitary for *GnRHR, GnIHR, PRL, FSH, LH, PRLR*, respectively. (J, K) Western blot analysis of GnRH and GnIH protein expression of hypothalamus.

(Figures 4H and 4I). Additionally, hypothalamic *TRH* mRNA expression (Figure 4E) was highest on d 13, which was significantly higher than on d 45, and the gene expression levels on d 0 and 27 were similar and centered. Pituitary *TSHβ* mRNA (Figure 4F) was expressed at the highest level on d 13, with similar expression levels on d 0, while on d 27 and 45 *TSHβ* expression was highly significantly lower ($P <$ 0.01). The pituitary *TSHR* mRNA expression level (Figure 4G) was highest on d 0 and decreased sharply with the extension of test time, showing highly significant differences on d 13, 27, and 45 ($P < 0.01$).

DISCUSSION

Most birds are seasonal breeding animals, and the change of the light photoperiod is an important driver of their seasonal breeding (Dawson et al., 2001; Kang and Kuenzel, 2015). The Magang goose is a typical representative of goose species in south China, and also a typical short-day breeder. Long light inhibits its reproductive activity while short light promotes reproductive activity (Huang et al., 2008; Qin et al., 2013; Lei et al., 2020). In the current experiment, the seasonal alteration of breeding activities of Magang geese was successfully regulated
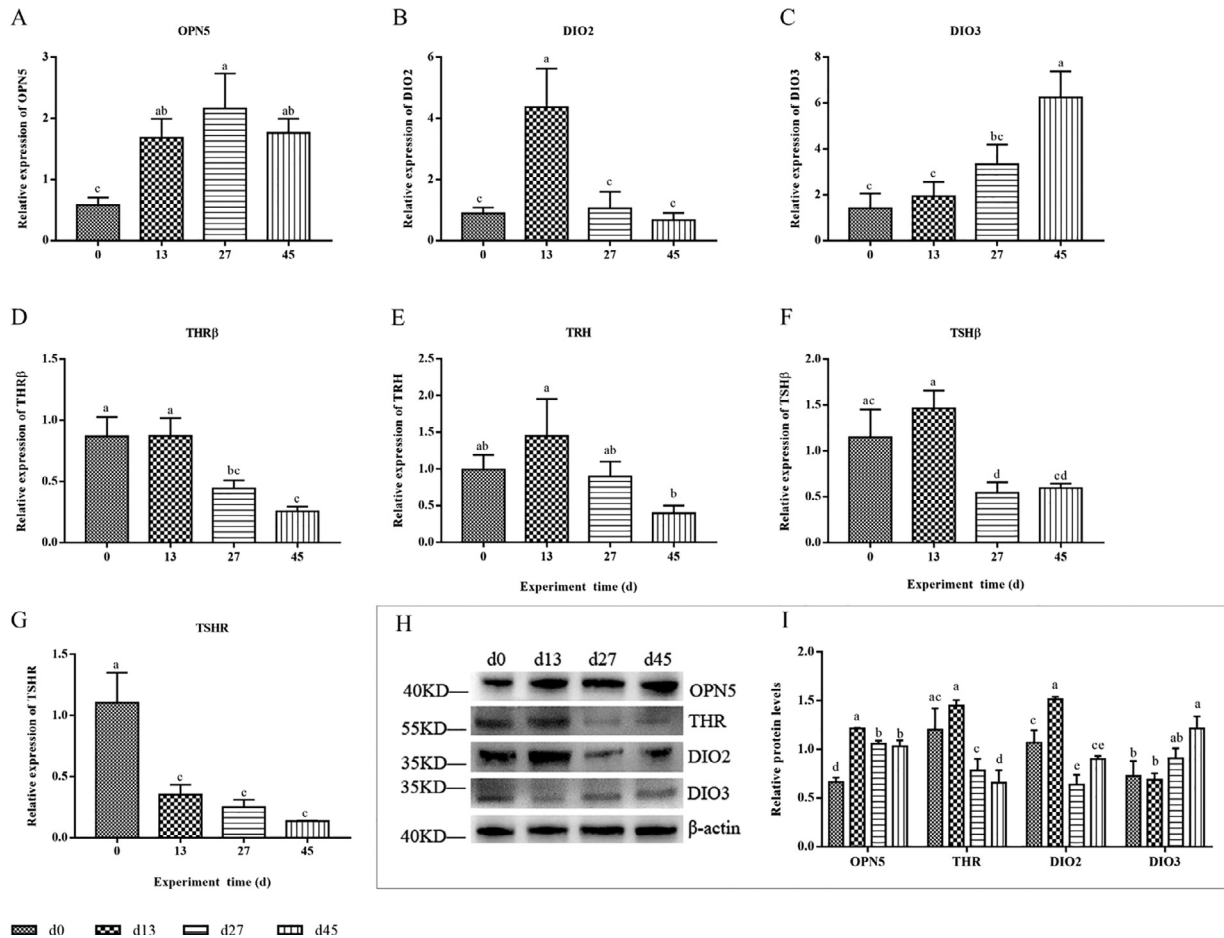
Figure 4. Expression of genes and proteins related to OPN5 and TSH-DIO2/DIO3 pathway. (A)The relative expression of hypothalamic *OPN5* mRNA. (B−E) The relative expression of hypothalamic *THRβ, DIO2, DIO3, TRH* mRNA, respectively. (F, G) The relative expression of *TSHβ* and *TSHR* mRNA of pituitary. (H, I) Western blot analysis of OPN5, THR, DIO2 and DIO3 protein expression of hypothalamus.

by an artificial light treatment, which again confirmed that light was the main regulatory factor of seasonal breeding activities of Magang geese, consistent with the results of previous studies (Shi et al., 2007; Huang et al., 2008). In the present study, when geese were exposed to a long-day photoperiod, the laying rate of female geese decreased gradually, and production stopped after 30 d. The testes of ganders also showed degeneration and atrophy on d 27 and 45. On d 0, the geese were in the reproductive phase and after extension of the photoperiod the geese started to enter the reproductive regression phase (d 1−30) and then enter the resting phase after 30 d. Previous studies (Shi et al., 2007; Huang et al., 2008) found that the egg laying of Magang geese increased briefly and then fell after the photoperiod was extended, which was not consistent with the egg laying observed in the current experiment.

Microscopic observation of testis histological sections also revealed that the spermatogenic function of the testis was normal on d 0 and 13, while degeneration occurred by d 27 and 45. This may be because the geese are relatively young and their reproductive system development is not sufficiently uniform. However, the changes of reproductive hormones in male geese showed a slight increase in serum testosterone, FSH, and LH concentrations on d 13, followed by a sharp decrease on

d 27 and 45 ($P < 0.01$), while PRL concentrations were low on d 0 and 13, and increased rapidly on d 27 and 45 ($P < 0.01$). The detection of HPG axis-related genes also revealed that *GnRH, GnRHR, FSH*, and *LH* were at high levels on d 0 and 13, and had decreased rapidly by d 27 and 45. In contrast, *GnIH, GnIHR, VIP, PRL*, and *PRLR* mRNA expression abundance was at a low level on d 0 and 13, and increased rapidly on d 27 and 45. In addition, GnRH protein expression was highest on d 13, with lower protein expression in the other 3 periods. GnIH protein levels increased gradually after the photoperiod was extended, and reached a peak on d 27. Studies have shown that the HPG axis is mainly regulated by hypothalamic GnRH and GnIH (Zhu et al., 2017; Dominoni et al., 2018; Dixit et al., 2020). GnRH binds to pituitary GnRHR and stimulates pituitary gonadotropin cells to synthesize and secrete FSH and LH, which eventually reach the testis through peripheral blood circulation and bind to specific receptors in the testis, respectively. FSH and FSHR combine to promote spermatogenesis, and the combination of LH and LHR regulates the secretion of steroid hormones and testicular development, while the increased secretion of steroid hormones (mainly testosterone) can inhibit the further release of GnRH, FSH, and LH. Studies on Magang geese found that a long-day photoperiod can promote

the expression and secretion of hypothalamus VIP and pituitary PRL, and inhibit the expression and secretion of GnRH and LH, while a short-day photoperiod has the opposite effect (Shi et al., 2007; Huang et al., 2008). Additionally, Gumułka and Rozenboim suggested that the plasma concentrations of testosterone and LH were significantly higher in geese under short-day conditions than that under long-day conditions, while PRL was significantly lower than under long light conditions (Gumułka and Rozenboim, 2015), which were consistent with the results of the present study.

OPN5 is one of the known deep brain photoreceptors, mainly located in the hypothalamic PVO (Nakane and Yoshimura, 2014; Pérez et al., 2019). It has been suggested that OPN5 at PVO transmits light information to the pars tuberalis (PT) and influences the secretion of TSH in the PT. TSH acts on the ependyrocytes of the hypothalamus and promotes the transformation of T4 into T3, which regulates the generation and secretion of GnRH/GnIH in the hypothalamus. Furthermore, seasonal reproductive activities are regulated by pituitary FSH and LH secretion (Yoshimura, 2010; Dixit and Byrsat, 2018; Renthlei et al., 2021). Studies in chicken, spotted munia, black-headed buntings, and Hungarian white geese (Kang and Kuenzel, 2015; Mishra et al., 2017, 2018; Zhu et al., 2019) suggest that long-day photoperiodic treatment stimulated the increase of OPN5 cell number and gene expression abundance. The present experiment also found that the expression of the OPN5 gene and protein increased with the extension of the photoperiod, which was consistent with the results of previous studies. The results for the TSH-DIO2/DIO3 pathway-related genes showed that the expression trends of hypothalamic $THR\beta$, $DIO2$, TRH, and pituitary $TSH\beta$ mRNAs were similar, with higher expression levels on d 0 and 13 and significantly lower expression levels in the 2 post-test periods (d 27 and45). $DIO2$, TRH, and $TSH\beta$ mRNA had the highest expression abundance on d 13, and hypothalamic DIO3 mRNA expression gradually increased throughout the experimental period, reaching the highest value on d 45. Moreover, the protein expressions of THR, $DIO2$, and $DIO3$ in the hypothalamus were consistent with the genes expression trend. The expression trend of pituitary $TSHR$ mRNA was completely opposite to that of $DIO3$, and the expression level was highest on d 0, and decreased significantly after that. The results were consistent with those reported in related studies.

Most studies have suggested that TSH is a master regulator of seasonal reproduction in birds (Ikegami and Yoshimura, 2012; Nakane and Yoshimura, 2014; Shinomiya et al., 2014; Guh et al., 2019). TSH stimulates tanycytes lining the base of the third ventricle and activates DIO2 in the ependymal which enhances T3 synthesis. T3 facilitates the release of gonadotropin-releasing hormone-I which stimulates reproductive activities (Kosonsiriluk et al., 2013). Intracerebroventricular injection (**ICV**) of TSH induces elevated testicular development and DIO2 expression and reduced DIO3 expression in short-day exposed quail, and their testicular growth is almost the same as that in birds exposed to long daylight (Nakao et al., 2008). But the genes of the TSH-DIO2/DIO3 pathway respond to photoperiods differently in different birds. The knockdown of OPN5 is via small interfering RNA antisense in the MBH promoted $TSH\beta$ mRNA expression of adult border canaries (Stevenson and Ball, 2012). $OPN5$ mRNA expression was negatively correlated with that of $TSH\beta$ mRNA expression in redheaded buntings (Majumdar et al., 2015). Under short-daylight conditions (3L: 21D), the $OPN5$ and VIP levels of spotted munia decreased and $GnRH-1$ levels increased, while under long-day light conditions (21L:3D) the results were reversed (Mishra et al., 2018). However, ICV of OPN5 siRNA significantly reduced the number of OPN5-positive cells in the PVO, and suppressed the induction of $TSH\beta$ by long-day stimulus of UV light in eye-patched, pinealectomized quail. $DIO2$ expression was induced in MBH in a dose-dependent manner after ICV injection of TSH in quail under short-day conditions. In contrast, $DIO2$ expression was inhibited by ICV injection of $TSH\beta$ antibodies under long day conditions (Nakao et al., 2008). On d 3 and 7, $OPN5$ mRNA expression increased, as did TRH, $TSH\beta$, and $GNRH-1$, in chickens exposed to long-day photostimulation (Kang and Kuenzel, 2015). In a study of Yangzhou geese (Zhu et al., 2019), the expression of $OPN5$ was positively correlated with TSH and $DIO2$, and $OPN5$ was upregulated with long-day photoperiod exposure. Thus, the association between OPN5 stimulation and $TSH\beta$ has varied in different avian studies, and the specific mechanism of action remains to be determined. Still, the central molecular and cellular mechanisms between OPN5 and TSH in birds of different species may be different, which needs to be further studied.

CONCLUSIONS

Under long photoperiod conditions, the laying rate of female geese decreased, testicular function of ganders atrophied and degenerated, and the reproductive activity of geese was inhibited. When photoperiod increased, the mRNA and protein levels of OPN5 in hypothalamus were upregulated and the pituitary $TSH\beta$, TSHR, and hypothalamus $THR\beta$, TRH, and DIO2 were downregulated, which affected the expression of reproductive axis genes and secretion of serum reproductive hormones. These results suggest that OPN5 may be involved in photoperiodic signaling related to the neuroendocrine control of reproduction in the short-day breeding Magang goose via the TSH-DIO2 pathway, and that OPN5 exhibits inhibitory effects.

ACKNOWLEDGMENTS

DISCLOSURES

The authors declare no conflicts of interest.

REFERENCES

Banerjee, S., S. Shahin, and C. M. Chaturvedi. 2018. Age dependent variations in the deep brain photoreceptors (DBPs), GnRH-GnIH system and testicular steroidogenesis in Japanese quail, Coturnix coturnix japonica. Exp. Gerontol. 108:7–17.

Banerjee, S., and C. M. Chaturvedi. 2017. Testicular atrophy and reproductive quiescence in photorefractory and scotosensitive quail: involvement of hypothalamic deep brain photoreceptors and GnRH-GnIH system. J. Photochem. Photobiol. B 175:254–268.

Dardente, H., D. G. Hazlerigg, and F. J. P. Ebling. 2014. Thyroid hormone and seasonal rhythmicity. Front. Endocrinol. 5:19.

Dawson, A., V. M. King, G. E. Bentley, and G. F. Ball. 2001. Photoperiodic control of seasonality in birds. J. Biol. Rhythm 16:365–380.

Dixit, A. S., S. Byrsat, and N. S. Singh. 2020. Circadian rhythm in photoperiodic expressions of GnRH-I and GnIH regulating seasonal reproduction in the Eurasian tree sparrow, Passer montanus. J. Photochem. Photobiol. B 211:111993.

Dixit, A. S., and S. Byrsat. 2018. Photoperiodic control of GnRH-I expression in seasonal reproduction of the Eurasian tree sparrow. Photoch. Photobio. Sci. 17:934–945.

Dominoni, D. M., M. de Jong, M. Bellingham, P. O'Shaughnessy, K. van Oers, J. Robinson, B. Smith, M. E. Visser, and B. Helm. 2018. Dose-response effects of light at night on the reproductive physiology of great tits (Parus major): integrating morphological analyses with candidate gene expression. J. Exp. Zool. A 329:473–487.

García-Fernández, J. M., R. Cernuda-Cernuda, W. I. L. Davies, J. Rodgers, M. Turton, S. N. Peirson, B. K. Follett, S. Halford, S. Hughes, M. W. Hankins, and R. G. Foster. 2015. The hypothalamic photoreceptors regulating seasonal reproduction in birds: A prime role for VA opsin. Front. Neuroendocrin. 37:13–28.

Guh, Y., T. K. Tamai, and T. Yoshimura. 2019. The underlying mechanisms of vertebrate seasonal reproduction. Proc. Japan Acad. Series B 95:343–357.

Gumułka, M., and I. Rozenboim. 2015. Effect of breeding stage and photoperiod on gonadal and serotonergic axes in domestic ganders. Theriogenology 84:1332–1341.

Huang, Y. M., Z. D. Shi, Z. Liu, Y. Liu, and X. W. Li. 2008. Endocrine regulations of reproductive seasonality, follicular development and incubation in Magang geese. Anim. Reprod. Sci. 104:344–358.

Ikegami, K., and T. Yoshimura. 2012. Circadian clocks and the measurement of daylength in seasonal reproduction. Mol. Cell Endocrinol. 349:76–81.

Kang, S. W., and W. J. Kuenzel. 2015. Deep-brain photoreceptors (DBPs) involved in the photoperiodic gonadal response in an avian species, Gallus gallus. Gen. Comp. Endocr. 211:106–113.

Kojima, D., S. Mori, M. Torii, A. Wada, R. Morishita, Y. Fukada, and S. Yamazaki. 2011. UV-sensitive photoreceptor protein OPN5 in humans and mice. PLoS One 6:e26388.

Kosonsiriluk, S., L. J. Mauro, V. Chaiworakul, Y. Chaiseha, and M. E. El Halawani. 2013. Photoreceptive oscillators within neurons of the premammillary nucleus (PMM) and seasonal reproduction in temperate zone birds. Gen. Comp. Endocr. 190:149–155.

Kuenzel, W. J., S. W. Kang, and Z. J. Zhou. 2015. Exploring avian deep-brain photoreceptors and their role in activating the neuroendocrine regulation of gonadal development 1. Poult. Sci 94:786–798.

Lei, M., R. Chen, Q. Qin, H. Zhu, and Z. Shi. 2020. Transcriptome analysis to unravel the gene expression profile of ovarian follicular development in Magang goose. J. Reprod. Dev. 66:331–340.

Li, H., J. Proudman, and W. J. Kuenzel. 2009. Differential regulation of gene expression and release of FSH and prolactin by long day and sulfamethazine in chicks. Gen. Comp. Endocr. 161:262–266.

Liu, G. J., Z. F. Chen, X. H. Zhao, M. Y. Li, and Z. H. Guo. 2020. Meta-analysis: Supplementary artificial light and goose reproduction. Anim. Reprod. Sci. 214:106278.

Majumdar, G., S. Rani, and V. Kumar. 2015. Hypothalamic gene switches control transitions between seasonal life history states in a night-migratory photoperiodic songbird. Mol. Cell Endocrinol. 399:110–121.

Mishra, I., D. Singh, and V. Kumar. 2017. Seasonal alterations in the daily rhythms in hypothalamic expression of genes involved in the photoperiodic transduction and neurosteroid-dependent processes in migratory blackheaded buntings. J. Neuroendocrinol. 29, doi:10.1111/jne.12469.

Mishra, I., N. Agarwal, S. Rani, and V. Kumar. 2018. Scotostimulation of reproductive neural pathways and gonadal maturation are not correlated with hypothalamic expression of deiodinases in subtropical spotted munia. J. Neuroendocrinol. 30:e12627.

Mohsin, A. Z., R. Sukor, J. Selamat, A. S. Meor Hussin, I. H. Ismail, N. N. Jambari, and F. Mustaffa-Kamal. 2020. Generation of high affinity anti-peptide polyclonal antibodies recognizing goat αs1-casein. Molecules 25:2622.

Nakane Yusuke, Y. T. 2019. Photoperiodic regulation of reproduction in vertebrates. Anim. Biosci. 7:173–194.

Nakane, Y., K. Ikegami, H. Ono, N. Yamamoto, S. Yoshida, K. Hirunagi, S. Ebihara, Y. Kubo, and T. Yoshimura. 2010. A mammalian neural tissue opsin (Opsin 5) is a deep brain photoreceptor in birds. Proc. Natl. Acad. Sci. 107:15264–15268.

Nakane, Y., T. Shimmura, H. Abe, and T. Yoshimura. 2014. Intrinsic photosensitivity of a deep brain photoreceptor. Curr. Biol. 24: R596–R597.

Nakane, Y., and T. Yoshimura. 2014. Universality and diversity in the signal transduction pathway that regulates seasonal reproduction in vertebrates. Front. Neurosci.-Switz 8:115.

Nakao, N., H. Ono, T. Yamamura, T. Anraku, T. Takagi, K. Higashi, S. Yasuo, Y. Katou, S. Kageyama, Y. Uno, T. Kasukawa, M. Iigo, P. J. Sharp, A. Iwasawa, Y. Suzuki, S. Sugano, T. Niimi, M. Mizutani, T. Namikawa, S. Ebihara, H. R. Ueda, and T. Yoshimura. 2008. Thyrotrophin in the pars tuberalis triggers photoperiodic response. Nature 452:317–322.

Pérez, J. H., E. Tolla, I. C. Dunn, S. L. Meddle, and T. J. Stevenson. 2019. A comparative perspective on extra-retinal photoreception. Trend Endocrinol. Metab. 30:39–53.

Qin, Q., A. Sun, R. Guo, M. Lei, S. Ying, and Z. Shi. 2013. The characteristics of oviposition and hormonal and gene regulation of ovarian follicle development in Magang geese. Reprod. Biol. Endocrinol. 11:65.

Renthlei, Z., L. Hmar, and T. A. Kumar. 2021. High temperature attenuates testicular responses in tree sparrow (Passer montanus). Gen. Comp. Endocrinol. 301:113654.

Shi, Z. D., Y. M. Huang, Z. Liu, Y. Liu, X. W. Li, J. A. Proudman, and R. C. Yu. 2007. Seasonal and photoperiodic regulation of secretion of hormones associated with reproduction in Magang goose ganders. Domest. Anim. Endocrinol. 32:190–200.

Shichida, Y., and T. Matsuyama. 2009. Evolution of opsins and phototransduction. Phil. Trans. Royal Soc. B: 364:2881–2895.

Shinomiya, A., T. Shimmura, T. Nishiwaki-Ohkawa, and T. Yoshimura. 2014. Regulation of seasonal reproduction by hypothalamic activation of thyroid hormone. Front. Endocrinol. 5:12.

Stevenson, T. J., and G. F. Ball. 2012. Disruption of neuropsin mRNA expression via RNA interference facilitates the photoinduced increase in thyrotropin-stimulating subunit β in birds. Eur. J. Neurosci. 36:2859–2865.

Tamai, T. K., and T. Yoshimura. 2017. Molecular and neuroendocrine mechanisms of avian seasonal reproduction. Adv. Exp. Med. Biol. 1001:125–136.

Van Wyk, B., and G. Fraley. 2021. Ontogeny of OPN4, OPN5, GnRH and GnIH mRNA expression in the posthatch male and female Pekin Duck (Anas platyrhynchos domesticus) suggests OPN4 may have additional functions beyond reproduction. Animals 11:1121.

Yoshimura, T. 2010. Neuroendocrine mechanism of seasonal reproduction in birds and mammals. Anim. Sci. J. 81:403–410.

Zhu, H. X., M. D. Hu, B. B. Guo, X. L. Qu, M. M. Lei, R. Chen, Z. Chen, and Z. D. Shi. 2019. Effect and molecular regulatory mechanism of monochromatic light colors on the egg-laying performance of Yangzhou geese. Anim. Reprod. Sci. 204:131–139.

Zhu, H. X., X. Q. Liu, M. D. Hu, M. M. Lei, Z. Chen, S. J. Ying, J. N. Yu, Z. C. Dai, and Z. D. Shi. 2019. Endocrine and molecular regulation mechanisms of the reproductive system of Hungarian White geese investigated under two artificial photoperiodic programs. Theriogenology 123:167–176.

Zhu, H., Z. Chen, X. Shao, J. Yu, C. Wei, Z. Dai, and Z. Shi. 2017. Reproductive axis gene regulation during photostimulation and photorefractoriness in Yangzhou goose ganders. Front. Zool. 14:11.